Real Time Optimal Control of Supercapacitor Operation for Frequency Response

IEEE Power & Energy Society General Meeting (2016)

Yusheng Luo, Mayank Panwar, Manish Mohanpurkar, Rob Hovsapian

July 2016

The INL is a U.S. Department of Energy National Laboratory operated by Battelle Energy Alliance



This is a preprint of a paper intended for publication in a journal or proceedings. Since changes may be made before publication, this preprint should not be cited or reproduced without permission of the author. This document was prepared as an account of work sponsored by an agency of the United States Government. Neither the United States Government nor any agency thereof, or any of their employees, makes any warranty, expressed or implied, or assumes any legal liability or responsibility for any third party's use, or the results of such use, of any information, apparatus, product or process disclosed in this report, or represents that its use by such third party would not infringe privately owned rights. The views expressed in this paper are not necessarily those of the United States Government or the sponsoring agency.

Real Time Optimal Control of Supercapacitor Operation for Frequency Response

Yusheng Luo*, Mayank Panwar[†], Manish Mohanpurkar* and Rob Hovsapian*

*Idaho National Laboratory, Idaho Falls, ID 83415

{yusheng.luo, manish.mohanpurkar, rob.hovsapian}@inl.gov

[†]Colorado State University, Fort Collins, CO 80523

mayank@rams.colostate.edu

Abstract-Supercapacitors are finding wider applications in modern power systems due to a controllable fast dynamic response. Use of power electronically interfaced supercapacitors for frequency support is a proven technique. In practical applications the heat generated from the Equivalent Series Resistance (ESR) can significantly reduce the life of supercapacitor. Hence thermal issues must be addressed for optimal operation. It is infeasible to use traditional optimization control methods to mitigate the impacts of frequent cycling due to the lack of active thermal management. This paper proposes a Front End Controller (FEC) using Generalized Predictive Control based on real time receding optimization. The constraints in the optimization are based on thermal management to enhance the efficiency of utilization life of the supercapacitors. A rigorous mathematical derivation is provided and supporting simulation results are obtained using Real Time Digital Simulator to demonstrate the effectiveness of the proposed technique.

Keywords—Supercapacitors, Front End Controller, Generalized Predictive Control, Receding Optimization, Real Time Digital Simulator.

I. INTRODUCTION

The increasing demand for reducing fossil fuel consumption has led to the trend of increasing utilization of renewable energy resources [1], [2]. Compared with traditional fossil fuel generation, renewable energy resources have the advantages of less carbon emission, environmental friendly, and lower cost of operation [3], [4]. However, a spatiotemporal variability in the renewable energy resources makes them non-dispatchable. To reduce impact of this output variability, Energy Storage (ES) can serve as a reservoir of energy, which can store excess generation during low load period and inject power back to the grid during high load demand [5].

ESs have diverse forms of physical realizations and operational characteristics [6]. Due to differences in physical configurations, technologies, and densities of power and energy, optimal control is non-trivial [7]. Applications of ESs in power systems varies widely based on its characteristics and need [8]. Battery ES is mainly used to reduce the operation cost of storage, due to its high energy density [9]. However, due to its slow response speed, it cannot provide frequency support. Flywheels can be considered as a medium-fast response ES, which is a tradeoff between higher energy and power density [7]. Supercapacitors feature a fast charging/discharging characteristic that can satisfy a power density application [10].

In [11], the authors presented methods to mitigate the impact of fixed charging time of a supercapacitor in ship-

board microgrid. The proposed control algorithm required deep understanding of the system parameters in order to set a proper fixed charging time. On account of the differences in configuration of the shipboard power system and traditional terrestrial power system, this approach is not readily adoptable. In [12]-[14], supercapacitors are integrated with wind turbine and photovoltaic in order to support the constant power operation of renewable generation. In [15], [16], a detailed model of supercapacitor was developed with close loop control with superior tracking performance. In [17], the power electronics interface of supercapacitor was described that can enable efficient cohesive operation of supercapacitor and other ES technologies. In [18], the impact of charging supercapacitors in a distribution system was analyzed and its advantages were demonstrated. In [19], [20], supercapacitors controllers were developed according to different operational scenarios, such as maintaining voltage stability and tracking step load change. However, none of the proposed controllers account for thermal management of supercapacitors operation.

This paper proposes a Front End Controller (FEC) employing Generalized Predictive Control (GPC) algorithm to control the charging/discharging of ES in a simplified, notional microgrid. GPC based FEC executes receding optimization according to the real time feedback of signal for various aspects such as system stability, supercapacitor thermal condition, remaining stored energy, etc. This provides the reference for power electronics interface charging/discharging under optimal thermal and electrical conditions of operation.

II. SYSTEM DESCRIPTION

A. Microgrid with Supercapacitor Energy Storage

A configuration of notional microgrid with Supercapacitor Energy Storage (SES) is shown in Fig. 1. In this system, a Permanent Magnet Synchronous Generator (PMSG) serves as the main power source. Its real and reactive power is adjusted by Prime Mover (PM) and Voltage Regulator (VR), respectively. Besides the PMSG module, there exists a SES module connected to the distribution bus via Power Electronics Interface (PEI) and a hybrid dynamic load, which is a combination of diverse types of loads such as resistive loads, inductive load, pulsed power loads, etc. A 4.15 kV AC distribution feeder connects the PMSG, SES, and hybrid dynamic load.

The major role of SES in this system is to provide real power compensation in order to assist the PMSG to maintain frequency stability. When the frequency drops beyond the

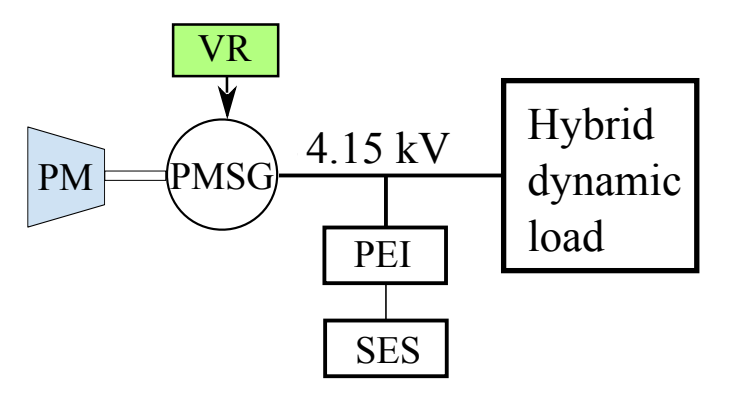


Fig. 1. Microgrid With Supercapacitor Energy Storage

system nominal value, it is expected to vary the real power generation according to swing equation [21].

The PEI, as shown in Fig. 2, is formed by a bi-directional AC/DC rectifier/inverter, a buckboost DC/DC chopper, and controller. PEI controller contains two hierarchical components i.e., FEC and lower level controller. FEC generates the expected value of PEI output based on feedback of PEI output, SES temperature, microgrid optimized system state variables, etc. With the acquired information, FEC performs optimization to compute the achievable power output value. This value from FEC will be sent to the next level as the reference signal. The low level controller will drive the power output of PEI and track the reference signal. The state-of-the-art technology for low level controller is matured and widely available, however FEC and its functionalities is a technical gap. This paper focuses on bridging this gap through the development of FEC that can generate optimal reference signal for low level controller.

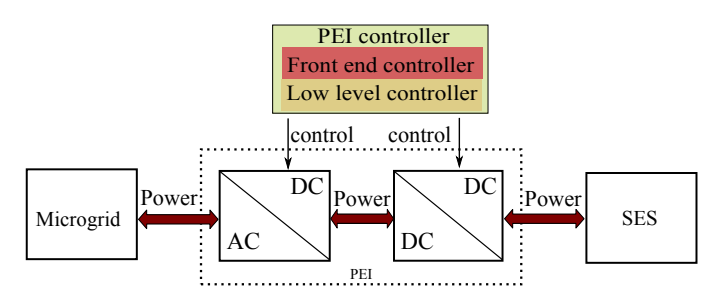


Fig. 2. Configuration of Supercapacitor Energy Storage

B. Problem Statement

In a microgrid, impedance of the load connected to the distribution bus is time dependent [22]. It is a challenge to precisely estimate the contribution from SES under dynamic grid conditions. During the practical operation of SES, thermal management is another critical issue that cannot be ignored as noted earlier. All the aforementioned variables change dynamically and are difficult to predict even few minutes ahead. Thus the classical control method based on overall optimization does not fit the requirement of SES operation.

C. Generalized Predictive Control

GPC is one of the model predictive control methods developed for controlling object operating in noisy and time variant

condition. It calculates control signal based on a simplified model of the plant. The feedback provides guidance for tuning the underlying model of the controlled object. GPC allows use of receding optimization for effective generation of control signal. In this paper, receding optimization is performed based on the real time information input for every control cycle. Therefore the generated optimal control signal can better reflect the real time condition of the system state. The successful control of GPC relies heavily on the fast I/O and computation of controller. With the development of digital signal processors, fast switchable semiconductor technology, and rapid computations make the practical implementation of such a framework possible. In the study presented in this paper, GPC will generate the real time optimal power reference signal based on the information, such as remaining stored energy, current supercapacitor temperature, and system frequency.

III. GPC FOR SES OPERATION CONTROL

A. Controlled Auto-Regressive and Integrated Moving-Average Model

GPC algorithm employs CARIMA (Controlled Auto-Regressive and Integrated Moving-Average) model, which can better inhibit the noise caused by random steps occurring at random times and Brownian motion. Those two noise sources are prevalent in a practical environment of SES [23]. To apply the GPC, development of a CARIMA model is the first step. The deviation of frequency is denoted by:

$$\dot{f} = \frac{f_0}{2D_{kin0}} \left[\sum_{i=1}^{m} (P_{G_i}) - P_L \right]. \tag{1}$$

Where, P_{G_i} is the real power output of ith source, m is the total number of sources, P_L is the sum of total real power consumption, f_0 is the system nominal frequency, D_{kin0} is the initial kinetic energy of the generators. It is difficult to decide D_{kin0} for a fixed value, because it changes with the system state and time. During steady state operating conditions, the instant value of ω_{kin0} can be calculated from the measurement data. Let the constant α as:

$$\alpha = \frac{f_0}{2D_{kin0}},\tag{2}$$

By defining a variable P as:

$$P = \sum_{i=1}^{m} (P_{G_i}) - P_L, \tag{3}$$

Linearizing (1):

$$\dot{f} = \alpha P. \tag{4}$$

Discretizing (4):

$$\frac{f_{k+1} - f_k}{T} = \alpha P_k. \tag{5}$$

Where k is the time variable, and T is the time step.

Deriving the expression of f_{k+1} from (5):

$$f_{k+1} - f_k = \alpha T P_k, \tag{6}$$

$$f_{k+1}(1 - q^{-1}) = \alpha T P_k, \tag{7}$$

$$f_{k+1}(1-q^{-1}) = \alpha T P_k + \frac{C(q^{-1})\xi(t)}{\Lambda}.$$
 (8)

Where, $C(q^{-1})=1+c_1q+\cdots+c_{nc}q^{-nc}$, $\xi(t)$ is a stochastic time signal, and Δ is the differencing operator $1-q^{-1}$. The product of these three terms represents the stochastic noise. Equation (8) denotes the CARIMA model of the system frequency deviation.

B. Generating Control Signal

Based on the CARIMA model, the controller based on GPC is developed. Since the stochastic signal cannot be predicted, during the development of controller, stochastic noise in (8) is ignored. Following the derivation procedure in [23], the relation between the current input P_k with the future output f_{k+j} can be expressed in (9):

$$\hat{f} = G\tilde{P} + h,\tag{9}$$

Where.

$$\hat{f} = [f_{k+1}, f_{k+2}, \cdots, f_{k+N}]^T,$$

$$\tilde{P} = [\Delta P_k, \Delta P_{k+1}, \cdots, \Delta P_{k+N-1}]^T,$$

$$h = [h_{k+1}, h_{k+2}, \cdots, h_{k+N}]^T.$$

 f_{k+1} , $j=1,\cdots,N$, represents the future value of system frequency. N is the predicting window, here we set it as three. G is the coefficient matrix. The expression of G in the study of this paper is derived as:

$$G_3 = \begin{bmatrix} \alpha T & 0 & 0 \\ 2\alpha T & \alpha T & 0 \\ 3\alpha T & 2\alpha T & \alpha T \end{bmatrix}.$$

 ΔP_{k+j-1} , $j=1,\cdots,N$, represents the input time series. GPC does not calculate the expected future input value, instead it calculates the expected increment of the future input based on the current input as seen in (9). h_{k+j} , $j=1,\cdots,N$, is a term developed for prediction. The expression is:

$$h_{k+1} = 2f_k - f_{k-1},$$

$$h_{k+2} = 3f_k - 2f_{k-1},$$

$$h_{k+3} = 4f_k - 3f_{k-1}.$$

For a known ΔP_{k+j-1} , f_{k+1} can be predicted. Thus the objective function for GPC based controller is:

$$J = [(G\tilde{P} + h - \omega)^T (G\tilde{P} + h - \omega) + \lambda \tilde{P}^T \tilde{P}].$$
 (10)

 ω is the expectation of frequency f_{k+1} , $j=1,\cdots,N$. The objective is to minimize the difference between f and ω , and inhibit the increment of P as well. The minimum value of the objective function is computed by equating the first time derivative with zero as shown in (11):

$$\dot{J} = 2[(G^TG + \lambda I)\tilde{P} - G^T(\omega - h)] = 0. \tag{11}$$

The value of optimal input increment is:

$$\tilde{P} = [(G^T G + \lambda I)^{-1} G^T (\omega - h)]. \tag{12}$$

Calculating the optimal value of ΔP_{k+j-1} using the expectation ω from (12).

$$\Delta P = \sum_{i=1}^{m} \Delta P_{G_i} - \Delta P_L. \tag{13}$$

 $\Delta P_{k+j-1} = \Delta P_{SES}$ is set at the first step, assuming the fast sampling rate and control action can overcome lack of generation and load information. This assumption is verified in the following section via simulation results.

C. Receding Optimization for SES Current under Thermal Constraint

In power systems, the requirement of maintaining system frequency is rigid and hence large deviations must be avoided during operation. Therefore, the expectation will always be set to the nominal frequency f_0 , based on which we compute the expected increment ΔP_{k+j-1} . The increment of SES output ΔP_{k+j-1} is constrained by the thermal conditions.

Table I lists the Equivalent Series Resistance (ESR) of the supercapacitor hardware from an OEM. Due to the existence of ESR, operating current will produce non-zero heat. Temperature rise resulting from the generated and accumulated heat may shorten the life of supercapacitor on account of cycling. Therefore thermal management is comprehensively considered for both charging and discharging. A supercapacitor matrix with a total equivalent capacitance of 100 Farad and 0.35 m Ω ESR is used in this simulation. The maximum voltage that can be stored in the capacitor is 5 kV. Fig. 3 indicates a significant reduction in the operational life of SES in case the operating temperature is high. Maximum allowable temperature (T_{max}) equal to 30 °C is used as a constraint to optimize the SES current.

Suppose the thermal capacitance of the selected supercapacitor in this research is 410 J/°C. This implies that 410 J heat generated by ESR can increase its temperature by 1 °C without any cooling. Based on the power output and temperature on supercapacitor, the allowed power increment will be calculated simultaneously with power increment focusing on maintaining nominal frequency. The power consumed on ESR with both methods will be compared and discussed. Based on the instantaneous and maximum allowable temperature, the maximum heat that will be generated from the next SES operation is calculated. For the temperature to rise from 25 °C (ambient temperature) to T_{max} is $(T_{max} - 25) \times 410$ J. By setting an allowed temperature rise time $t_{rise,0}$, which is the shortest allowed time for temperature to rise from 25 °C to T_{max} . In case the operating temperature becomes T_{max} , the SES current drops to zero following a fixed slope expressed as:

$$I_c = b - \frac{bt}{t_{rise,0}}. (14)$$

The heat generated due to SES operation that leads to a temperature increase from 25 °C to T_{max} is given below:

$$ESR \int_{0}^{t_{rise,0}} (b - \frac{b}{t_{rise,0}} t)^{2} dt = (T_{max} - 25) \times 410.$$
 (15)

Equation (15) is solved to obtain the value of b used in (14). According to (15), each value of temperature between 25 $^{\circ}$ C

TABLE I. ESR VALUES FOR A PRACTICAL SUPERCAPACITOR [24]

Capacitance (Farad)	650	1200	1500	2000	3000
ESR (mΩ)	0.8	0.58	0.47	0.35	0.29

and T_{max} has a unique mapping value of t_{rise} resulting from (14). Therefore, by replacing the T_{max} with the instantaneous temperature T as:

$$ESR \int_{0}^{t_{rise}} (b - \frac{b}{t_{rise,0}} t)^{2} dt = (T - 25) \times 410, \quad (16)$$

The value of t_{rise} is computed by solving (16), which is used in (14) provides maximum allowable magnitude of SES current for the next time step. In this manner, the computed reference signal from GPC will be limited by the thermal constraints.

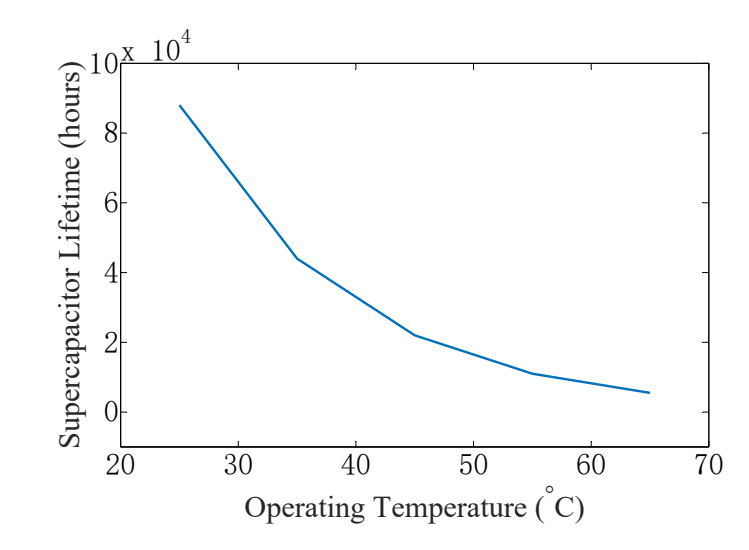


Fig. 3. Sample Curve of Supercapacitor Lifetime vs Temperature [24]

IV. REAL TIME SIMULATION RESULTS

To verify the performance of the proposed control strategy, simulations are performed in a real time environment. Real time models of the FEC, lower level controller, PEI, SES, and the microgrid are implemented. The typical simulation time step for this setup is 50 μ s and the small time step (controls and PEI) ranges from 2.5 to 4 μ s in real time. In the simulation, the rating of PMSG is 45 MVA and the initial voltage of SES is 4 kV. A 9 MW resistive load is brought online as a unit step load while the output of PMSG is 10 MW. For this unit step load, system frequency response and operational temperature of SES under three scenarios are shown in Figs. 4 and 5, respectively.

In the first scenario, there is no power compensation from SES and Fig. 4 shows the system frequency drops below 59.4 Hz. This frequency deviation exceeds 1% of the nominal frequency. In the second test scenario, an SES controlled by GPC is implemented without any thermal constraints. Fig. 4 indicates that the frequency is maintained above 59.85 Hz in this scenario. However Fig. 5 indicates that the final

temperature reaches up to 32 °C for this cycle. In the third test scenario, an SES controlled by GPC considering thermal constraint is implemented with $t_{rise,0}$ as 50 seconds and T_{max} as 30 °C. In this scenario, the system frequency is maintained above 59.5 Hz and the SES temperature is maintained below 28 °C. According to the test results, the proposed control strategy can achieve a balance between maintaining system frequency and limiting SES temperature below a desired value.

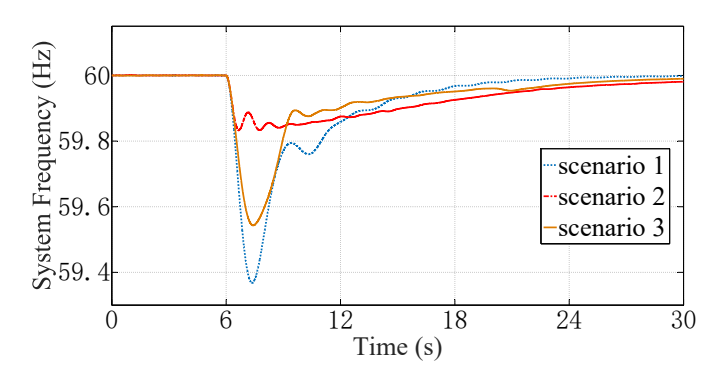


Fig. 4. System Frequency Response in Scenarios 1, 2, and 3

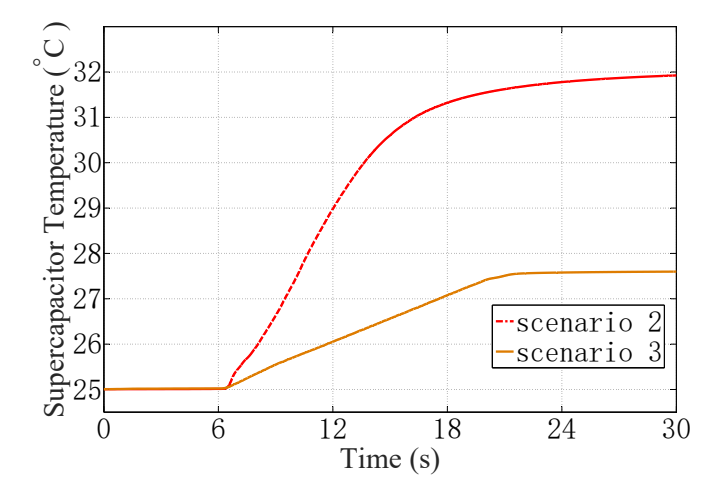


Fig. 5. SES Temperature in Test Scenarios 2 and 3

V. CONCLUSION

In this paper, a novel Generalized Predictive Control considering thermal constraint for supercapacitor energy storage is proposed and its effectiveness is demonstrated. Test result shows the proposed control strategy can achieve both frequency support and optimal thermal management goals. A real time simulation of the supercapacitor, power electronics, a novel front end controller, and lower level controller is created and its optimal operation is demonstrated. The test results can provide reference for developing cooling system to enable economic and effective cooling. Future work involves using supercapacitor hardware for performing Hardware-in-the-Loop (HIL) verification tests for controller rapid-prototyping in real time environment. Developing effective cooling system and implementing optimization to achieve higher SES utilization and economic cooling are additional avenues of future work.

ACKNOWLEDGEMENT

This work has been supported by the Laboratory Directed Research and Development funds, Energy and Environment Science and Technology (EE S&T) Directorate, Idaho National Laboratory (INL) and Fuel Cell Technology Office, Department of Energy.

REFERENCES

- [1] S. Salinas, M. Li, P. Li, and Y. Fu, "Dynamic energy management for the smart grid with distributed energy resources," *IEEE Trans. Smart Grid*, vol. 4, no. 4, pp. 2139–2151, Dec 2013.
- [2] L. L. Lai and T. F. Chan, Distributed generation: Induction and permanent magnet generators. John Wiley & Sons, 2008.
- [3] F. Katiraei, R. Iravani, N. Hatziargyriou, and A. Dimeas, "Microgrids management," *IEEE Power and Energy Maga.*, vol. 6, no. 3, pp. 54–65, May 2008.
- [4] J. Zhao, K. Graves, C. Wang, G. Liao, and C.-P. Yeh, "A hybrid electric/hydro storage solution for standalone photovoltaic applications in remote areas," in *Proc. IEEE Power and Energy Society General Meeting*, San Diego, CA, 2012, pp. 1–6.
- [5] J. Barton and D. Infield, "Energy storage and its use with intermittent renewable energy," *IEEE Trans. Energy Conversion*, vol. 19, no. 2, pp. 441–448, June 2004.
- [6] M. Molina, "Distributed energy storage systems for applications in future smart grids," in *Proc. 6th IEEE/PES Transmiss. and Distrib. Latin Amer. Conf. Exposit.*, Sept 2012, pp. 1–7.
- [7] J. W. Shim, Y. Cho, S.-J. Kim, S. W. Min, and K. Hur, "Synergistic control of smes and battery energy storage for enabling dispatchability of renewable energy sources," *IEEE Trans. Applied Superconductivity*, vol. 23, no. 3, pp. 5701 205–5701 205, June 2013.
- [8] V. Boicea, "Energy storage technologies: The past and the present," Proc. IEEE, vol. 102, no. 11, pp. 1777–1794, Nov 2014.
- [9] I. Miranda, N. Silva, and A. Maia Bernardo, "Assessment of the potential of battery energy storage systems in current european markets designs," in *Proc. International Conference on the European Energy Market (EEM)*, May 2015, pp. 1–5.
- [10] M. Winter and R. J. Brodd, "What are batteries, fuel cells, and supercapacitors?" *Chemical reviews*, vol. 104, no. 10, pp. 4245–4270, 2004
- [11] J. Crider and S. Sudhoff, "Reducing impact of pulsed power loads on microgrid power systems," *IEEE Trans. Smart Grid*, vol. 1, no. 3, pp. 270–277, Dec 2010.
- [12] L. Qu and W. Qiao, "Constant power control of dfig wind turbines with supercapacitor energy storage," *IEEE Trans. Industry Applications*, vol. 47, no. 1, pp. 359–367, Jan 2011.
- [13] C. Abbey and G. Joos, "Supercapacitor energy storage for wind energy applications," *IEEE Trans. Industry Applications*, vol. 43, no. 3, pp. 769–776, May 2007.
- [14] T. Zhou and W. Sun, "Optimization of battery-supercapacitor hybrid energy storage station in wind/solar generation system," *IEEE Trans.* Sustainable Energy, vol. 5, no. 2, pp. 408–415, April 2014.
- [15] H. El Fadil, F. Giri, J. Guerrero, and A. Tahri, "Modeling and nonlinear control of a fuel cell/supercapacitor hybrid energy storage system for electric vehicles," *IEEE Trans. Vehicular Technology*, vol. 63, no. 7, pp. 3011–3018, Sept 2014.
- [16] N. Rizoug, P. Bartholomeus, and P. Le Moigne, "Modeling and characterizing supercapacitors using an online method," *IEEE Trans. Industrial Electronics*, vol. 57, no. 12, pp. 3980–3990, Dec 2010.
- [17] D. Abeywardana, B. Hredzak, and V. Agelidis, "Single-phase grid-connected LiFePO₄ battery-supercapacitor hybrid energy storage system with interleaved boost inverter," *IEEE Trans. Power Electronics*, vol. 30, no. 10, pp. 5591–5604, Oct 2015.
- [18] Y. Luo, S. Srivastava, M. Andrus, and D. Cartes, "Application of distubance metrics for reducing impacts of energy storage charging in an mvdc based ips," in *Proc. Electric Ship Technologies Symposium* (ESTS), Arlington, VA, April 2013, pp. 287–291.

- [19] A. Rufer, D. Hotellier, and P. Barrade, "A supercapacitor-based energy-storage substation for voltage-compensation in weak transportation networks," in *Proc. IEEE Bologna, Power Tech Conference Proceedings*, vol. 3, June 2003, p. 8.
- [20] F. Inthamoussou, J. Pegueroles-Queralt, and F. Bianchi, "Control of a supercapacitor energy storage system for microgrid applications," *IEEE Trans. Energy Conversion*, vol. 28, no. 3, pp. 690–697, Sept 2013.
- [21] P. Kundur, N. J. Balu, and M. G. Lauby, *Power system stability and control*. McGraw-hill New York, 1994, vol. 7.
- [22] F. Magnago, L. Zhang, and R. Nagarkar, "Three phase distribution state estimation utilizing common information model," in *Proc. IEEE Eindhoven PowerTech*, June 2015, pp. 1–6.
- [23] D. W. Clarke, C. Mohtadi, and P. Tuffs, "Generalized predictive control part i. the basic algorithm," *Automatica*, vol. 23, no. 2, pp. 137–148, 1987
- [24] Datasheet: K2 ULTRACAPACITORS -2.7 SERIES, Maxwell Technology, 3888 Calle Fortunada, San Diego, CA 92123.